



Contents lists available at ScienceDirect

Journal of King Saud University – Science

journal homepage: www.sciencedirect.com

Original article

In vitro antidiabetic and anti-inflammatory effects of Fe-doped CuO-rice husk silica (Fe-CuO-SiO₂) nanocomposites and their enhanced innate immunity in zebrafish

G. Sabeena^a, S. Rajadurai^b, S.P. Mano bala^a, T. Manju^b, Hisham A. Alhadlaq^c, Raja Mohan^d, G. Annadurai^{a,*}, Maqusood Ahamed^{c,*}^a Sri Paramakalyani Centre of Excellence in Environmental Sciences, Manonmaniam Sundaranar University, Alwarkurichi 627412, India^b Sri Paramakalyani College, Manonmaniam Sundaranar University, Alwarkurichi 627412, India^c Department of Physics and Astronomy, College of Science, King Saud University, Riyadh 11451, Saudi Arabia^d Chemical Industry Research Institution, University of Ulsan, Ulsan 44776, South Korea

ARTICLE INFO

Article history:

Received 14 March 2022

Revised 11 April 2022

Accepted 21 May 2022

Available online 26 May 2022

Keywords:

Fe-doped CuO-SiO₂ nanocomposite

Rice husk

Antidiabetic effect

Anti-inflammatory activity

In vivo toxicity

Zebrafish

ABSTRACT

Recent studies are now focussing on synthesis of metal oxide based nanocomposites because of their exceptional physicochemical characteristics. In this study, CuO-SiO₂ nanocomposite (CuONC) and Fe-doped CuO-SiO₂ nanocomposite (FeCuONC) were synthesized by a simple hydrothermal method. XRD, SEM, EDX, FTIR, UV-vis, PSA, and TGA were utilized to confirm the synthesis of CuONC and FeCuONC. The *in vitro* biological activities and *in vivo* toxicity (zebrafish) of CuONC and FeCuONC were explored. The α -amylase assay showed that both CuONC, and FeCuONC exhibit dose-dependent antidiabetic activity. Interestingly, antidiabetic activity of FeCuONC was higher as compared to CuONC. Furthermore, FeCuONC showed higher anti-inflammatory effects (inhibition of denaturation of egg albumin) than those of CuONC. *In vivo* toxicity study in zebrafish embryos and larvae suggested that FeCuONC induce higher innate immunity response as compared to CuONC. Altogether, we observed that Fe-doped CuO-SiO₂ nanocomposites exhibited advance anti-inflammatory effect, sophisticated antidiabetic activity and enhanced innate immunity as compared to CuO-SiO₂ nanocomposite. This study warrants further research on therapeutic application of Fe-CuO-SiO₂ nanocomposites in suitable mammalian models.

© 2022 The Author(s). Published by Elsevier B.V. on behalf of King Saud University. This is an open access article under the CC BY-NC-ND license (<http://creativecommons.org/licenses/by-nc-nd/4.0/>).

1. Introduction

Nanostructures are being produced and explored for numerous applications worldwide (Ahamed et al., 2022a; Khan et al., 2021). Nanostructures display at least one dimension <100 nm, have been found to exhibit exceptional physicochemical characteristics than those of their bulk forms. The unique physicochemical properties of nanostructures hold great potential to improve economic and scientific aspects of human life ranging from agriculture, engineer-

ing and electronics to healthcare system and environmental remediation (Ahamed et al., 2022b). Silica nanoparticles (SiO₂ NPs) offer various biomedical applications such as drug delivery, biosensor, biomarker, and enzyme mobilization (Sazegar et al., 2017). There are several ways for the preparation of SiO₂ NPs. However, rice husk is an excellent precursor for SiO₂ NPs preparation (Jansomboon et al. 2017). SiO₂ is the major inorganic constituent of the rice husk (Liou and Yang, 2011). Leaching of rice husk by boiled and concentrated acid solutions is an effective method to remove most of the metallic impurities and getting white colored SiO₂ with a high specific surface area (Sharifnasab and Alamooti, 2017).

CuO NPs is the simplest member of the copper compounds family and possess unique characteristics e.g. spin dynamics, electron correlation effects, and high temperature superconductivity (Das et al., 2013). CuO NPs is being widely applied in sensor, solar energy, catalysis, and heat transfer fluids, and solar energy (Siddiqui et al., 2013). Due to a narrow bandgap energy, CuO NPs exhibit excellent photovoltaic and photocatalytic properties

* Corresponding authors.

E-mail addresses: gannadurai@msuniv.ac.in (G. Annadurai), mahamed@ksu.edu.sa (M. Ahamed).

Peer review under responsibility of King Saud University.



Production and hosting by Elsevier

<https://doi.org/10.1016/j.jksus.2022.102121>

1018-3647/© 2022 The Author(s). Published by Elsevier B.V. on behalf of King Saud University.

This is an open access article under the CC BY-NC-ND license (<http://creativecommons.org/licenses/by-nc-nd/4.0/>).

(Arfan et al., 2019). CuO NPs are also used in food containers and textiles because of their antimicrobial activity (Ahamed et al., 2014). However, wide-spread application of CuO NPs may raise concern of health hazard to the environment and humans. Leaching of Cu ions from the surface of CuO NPs plays crucial role in their toxicity (Ahamed et al., 2015). Doping with metal ions (e.g. Fe, Al, and Mn) could be a potential way to minimize the leaching of Cu ions from the surface of CuO NPs that make them safe for biomedical application. Besides, doping with transition metal ions might also tune the physical and chemical characteristics of CuO NPs that can be further applied in bioengineering. There are several available methods for successful synthesis of metal ions-doped metal oxide nanocomposites (Ahamed et al., 2021a; Subhalakshmi et al., 2019). In case of Fe-doped CuO NPs, the expected stronger binding interaction between Cu and Fe in the particle matrix could conceptually lead to decreased particle solubility in aqueous biological environments that potentially reduced toxicity (Naatz et al., 2017). It has also been reported that there is increase in oxidation activity of SiO₂ NPs following doping with Fe (Sazegar et al., 2017).

Recent studies are now focussing on synthesis of metal oxide based nanocomposites because of their superior characteristics in comparison to its individual material (Ahamed et al., 2021a; 2021b). There is little knowledge on biological applications and toxicity of Fe-doped CuO-SiO₂ nanocomposites. Keeping above point in mind, this study was designed to examine the several *in vitro* bioactivities and *in vivo* toxicity (zebrafish) of Fe-doped CuO-rice husk SiO₂ nanocomposites (FeCuONC) prepared by a simple hydrothermal method. The SiO₂ NPs (SNPs, from rice husk), CuO NPs, and CuO-SiO₂ nanocomposite (CuONC) were also prepared for comparison of physical, chemical, and biological properties from FeCuONC. X-ray diffraction (XRD), scanning electron microscopy (SEM), energy dispersive X-ray spectroscopy (EDX), Fourier transmission infrared (FTIR) microscopy, UV-vis spectrophotometer, particle size analyser (PSA), and thermogravimetric analysis (TGA) were applied for the characterization of synthesized samples. *In vitro* antidiabetic, anti-inflammatory, and antibacterial activity of prepared samples was examined. *In vivo* innate immunity of CuO-SiO₂ nanocomposite (CuONC) and Fe-doped CuO-SiO₂ nanocomposite (FeCuONC) in zebrafish embryos and larvae was also investigated. The zebrafish model offers several advantage over other model systems including ease of manual experimentation and drug administration and its prolific fertility (Garcia, et al., 2016). Zebrafish are easier and less expensive to house and care for as compared to rodent models (Kumari et al., 2017).

2. Experimental plan

2.1. Preparation of silica nanoparticles (SiO₂ NPs or SNPs) from rice husk

In first (I) process, raw rice husk (15 g) was washed in HCl solution (10 wt%) for refluxed 2 h, rinsed with deionized water, and then dried at 80 °C for 24 h. Sample was further calcined at 600 °C for 4 h to get white needle like crystals. In second (II) process, 2 g of white needle crystals were washed in HCl solution (10 wt%) for refluxed 2 h, rinsed with deionized water, and then dried at 80 °C for 24 h. After calcination (600 °C for 4 h) white ash formed. In third (III) process, 0.5 g of white ash added 15 ml of NaOH (1 N) solution for refluxed 2 h and centrifuged at 8000 rpm for 2 min. In the supernatant clear solution of Na₂SiO₃, the HCl (1 N) was added until get the pH 7. Sample was converted into silica gel and pyrolysis was carried out in a muffle furnace (80 °C for 2 h) to obtained silica (SiO₂) nanoparticles (SNPs). Fig. 1 displays the preparation procedures of SNPs from rice husk.

2.2. Synthesis of CuO NPs, CuO-SiO₂ nanocomposite (CuONC), and Fe-doped CuO-SiO₂ nanocomposite (FeCuONC)

For CuO NPs synthesis, 2.9 g of copper nitrate and 1.2 g of polyvinylpyrrolidone (PVP) were dissolved in 100 ml of distilled water with continuous stirring and heated the solution up to 600 °C. The NaOH solution (1 M) was further added dropwise with continuous stirring for 1 h to get black precipitate. Then mixture was centrifuged and dried at 80 °C for 1 h to get CuO NPs.

For CuO-SiO₂ nanocomposite (CuONC) synthesis, 1 g CuO NPs and 1 g SiO₂ NPs were mixed in 100 ml of distilled water and kept in shaker for 72 h. After that mixture was centrifuged at 2000 rpm for 20 min and dried at 80 °C for 1 h. Finally, sample was calcined at 600 °C for 4 h get blackish brown powder of CuONC.

For Fe-doped CuO-SiO₂ nanocomposite (FeCuONC) preparation, FeCl₃·6H₂O and CuO-SiO₂ in a concentration ratio of 1:6 was mixed in a beaker stirred for 1 h. Then, suspension was transferred into autoclave and heated at 180 °C for 3 h. After that suspension was centrifuged at 2000 rpm for 20 min and pellets were dried at 80 °C for 1 h. Finally, pellets were calcine at 600 °C for 4 h to get FeCuONC. Schematic of CuO NPs, CuONC, and FeCuONC synthesis is presented in Fig. 2.

2.3. Antidiabetic activity

Antidiabetic activity (α -amylase inhibition assay) of prepared samples was examined according to method described earlier (Sivashanmugam, 2017). Briefly, α -amylase (0.1 g in 100 ml of ice-cold distilled water) was mixed with different concentrations (10–50 μ g/mL) SNPs, CuONC, and FeCuONC and incubated for 10 min at 30 °C. Thereafter, starch substrate (0.55% in phosphate buffer) was added to start the reaction for 3 min. The reaction was terminated by adding 2 ml of DNS reagent (2% 3,5-dinitrosalicylic acid and 13% sodium potassium tartrate in 0.5 M NaOH) and was boiled for 10 min in a water bath at 90–100 °C. The mixture was cooled to room temperature and absorbance recorded at 540 nm using UV-visible spectrophotometer. The α -amylase inhibitory activity was expressed as percentage inhibition and was estimated using the following equation.

$$I_{\alpha\text{-Amylase}} (\%) = \frac{A_{540 \text{ Control}} - A_{540 \text{ Sample}}}{A_{540 \text{ Control}}} \times 100$$

2.4. Anti-inflammatory activity

The *in vitro* anti-inflammatory activity (inhibition of protein denaturation) was assessed as reported earlier (Nguemngang et al., 2019). In brief, 1 ml of aqueous solution of different concentrations (100, 200, 300, 400 and 500 μ g/mL) of SNPs, CuONC, and FeCuONC along with standard solution (diclofenac) was mixed with 1 ml of aqueous solution of bovine serum albumin (5%) and incubated at 37 °C for 15 min. Protein denaturation was carried out by placing the reaction mixture in a water bath at 80 °C for 10 min. Afterwards, mixture was cool down at room temperature and absorbance was measured at 660 nm by UV-visible spectrophotometer. The inhibition of protein denaturation was expressed as percentage inhibition and calculated using the following equation.

$$\% \text{ of inhibition} = \frac{\text{Absorbance}_{\text{Control}} - \text{Absorbance}_{\text{Sample}}}{\text{Absorbance}_{\text{Control}}} \times 100$$

2.5. Zebrafish maintenance

All the investigations were accomplished by standard animal practice of OECD guidelines for testing chemicals. Zebrafish (*Dania*

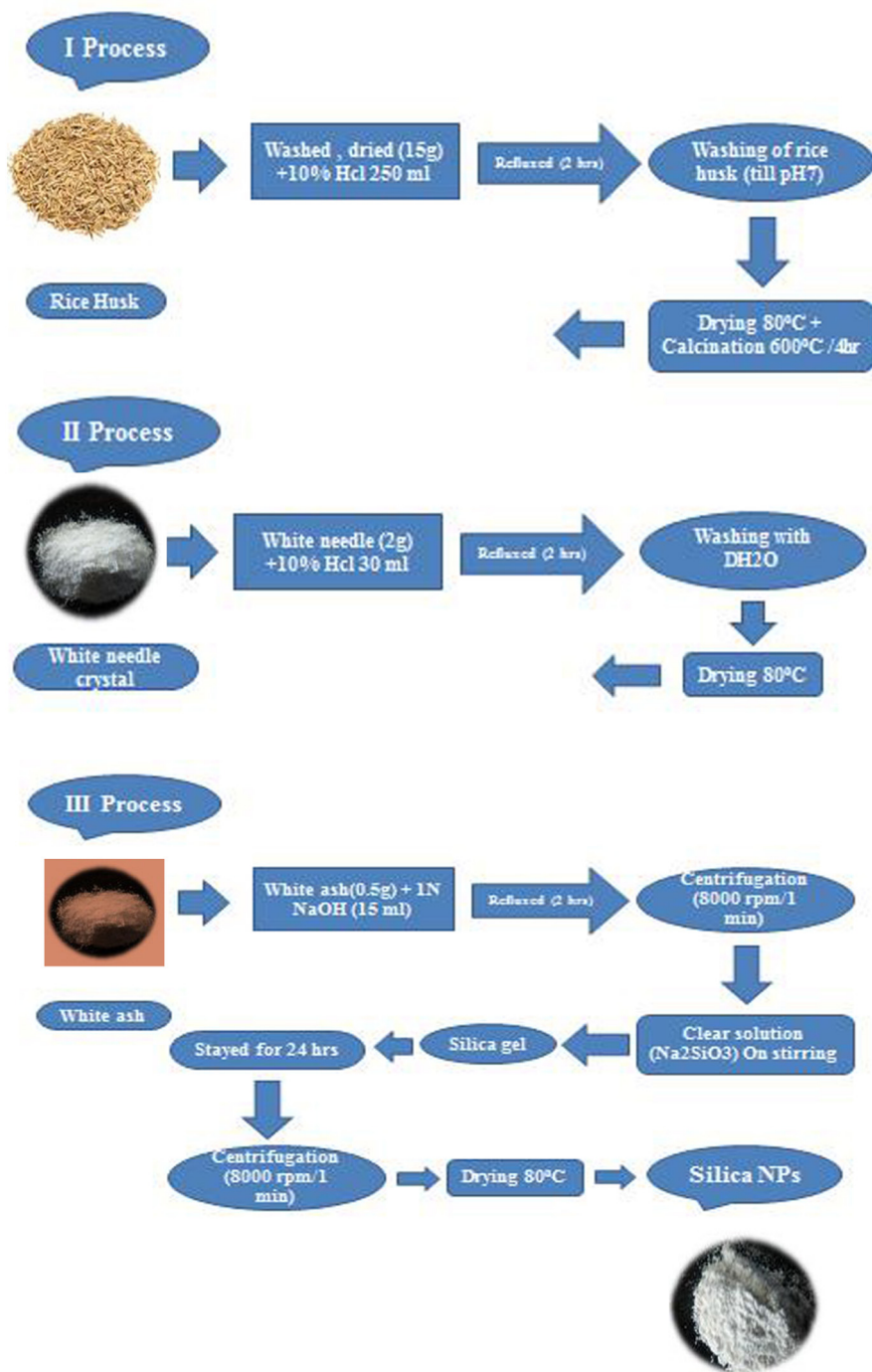


Fig. 1. Preparation of SiO₂ NPs (SNPs) from rice husk.

erio) were obtained from a native aquarium fish supplier (zebrafish wild-type AB strain). Zebrafish were maintained in wealth section loaded up with the adapted water (75 g NaHCO₃, 18 g ocean salt, 8.4 g CaSO₄, per 1000 L). Breeding of fishes was stimulated by sustaining female and male ratio of 3:1. Photo-periodic cycle was sustained by preserving them for 10 h dark and 14 h light. Eggs are collected in early morning and reared up in E3 medium (5 mM/L sodium chloride, 0.18 mM/L, potassium chloride, 0.33 mM/L, calcium chloride, and 0.33 mM/L magnesium sulfate) with 2 µg/mL gentamycin. The fish embryos were instigated from natural depositing and incubated at 28.5 °C.

2.6. Toxicity study of zebrafish embryos and larvae

In vivo toxicity of CuONC and FeCuONC was examined in zebrafish embryos and larvae. In brief, thirty zebrafish embryos of 24-hour post-fertilization (hpf) were exposed to different concentrations (25–200 µl) of CuONC and FeCuONC in E3 medium for 24, 48, 72, and 96 h. Microscopic observation was carried out at different time interval (24–96 h) to visualize the morphological abnormalities. The hatching rate, malformation, and embryos death were also determined. All the experiments were performed in triplicate.

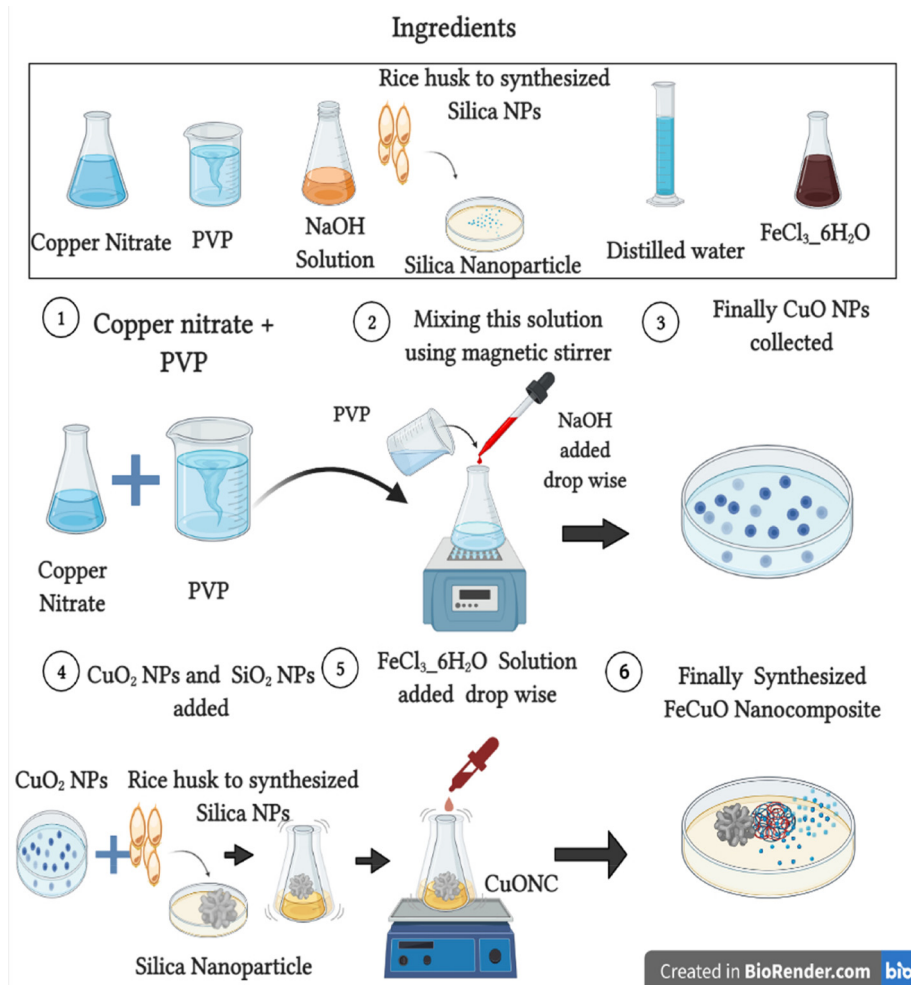


Fig. 2. Schematic of CuO NPs, CuONC, and FeCuONC synthesis.

3. Results and discussion

3.1. X-ray diffraction study

XRD spectra of prepared samples are presented in Fig. 3. The CuONC and FeCuONC exhibited the peaks at 32.6° , 35.6° , 38.8° , 48.7° , 53.5° , 58.5° , 61.6° , 66.3° , 68.3° , 72.5° , and 75.2° for the respective planes. Two highly intense diffraction peaks are observed at values 35.6° and 38.8° with a preferred orientation the (-111) and (111) axis and which can be indexed as monoclinic structure of CuO. Due to amorphous nature peak of SNPs was not appear in nanocomposite. Absence of Fe peak in FeCuONC suggested that Fe ions were homogeneously mixed with the nanocomposite. The average crystallite size was calculated from the peak width of most intense peak using Debye-Scherrer equation (Shahid et al. 2018). The average crystallite size of CuONC, and FeCuONC was around 36 nm, and 62 nm, respectively. Due to magnetic property Fe-doping might increase the agglomeration crystallites. This could be the possible reason of higher crystallite size of FeCuONC as compared to CuONC. Fe-doping might also increase the oxygen vacancies at the surface of FeCuONC that enhance its biological activities (Arfan et al., 2019).

3.2. FTIR analysis

FTIR spectra was recorded in the range of $500\text{--}4000\text{ cm}^{-1}$. The CuONC and FeCuONC show characteristic vibrations of monoclinic

CuO (Fig. 4). Presence of new band at 1738 cm^{-1} in FeCuONC in comparison to CuONC suggests new bond formation after Fe-doping. The 3011 cm^{-1} band of SNPs is due to the stretching vibration of O–H bonds in Si–OH and the HO–H of water molecules adsorbed on the surface (Adam et al. 2011). The Si–O–Si bond asymmetric stretching, symmetric and bending vibration were observed as reported in other studies (Rahman et al. 2009). In FTIR spectra of CuO– SiO_2 nanocomposite (CuONC), characteristic bands of SiO_2 were observed with marginal shifting of bands and slight changes in intensities of absorption bands at 1038 and 795 cm^{-1} (Farrukh et al. 2019). The absence of absorption modes related to secondary phases or other impurities confirms the successful Fe-doping in CuO– SiO_2 NC.

3.3. Optical characterization

Optical behavior of CuO– SiO_2 nanocomposite (CuONC) and Fe/CuO– SiO_2 nanocomposite (FeCuONC) was examined by UV-visible spectrophotometer. Fig. 5 represents the absorption spectra of CuONC and FeCuONC. The absorption peaks for CuONC were at 192 nm, 200 nm, 361 nm, and 376 nm while for FeCuONC were at 361 nm, 396 nm, and 576 nm. Two prominent peaks at 200 nm and 376 nm were assigned to the absorption of CuONC and two most prominent peaks at 361 nm and 576 nm were assigned to the absorption of FeCuONC (Das et al. 2013). Tauc plot shows that the bandgap energy of CuONC was decreased from 5.5 eV to 5.13 eV after Fe-doping.

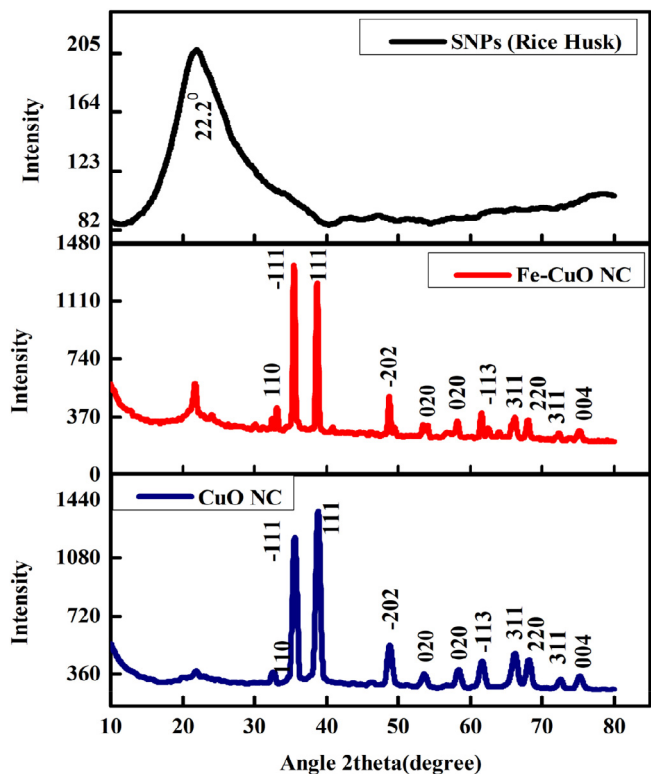


Fig. 3. XRD pattern of SNPs, CuO NC, and FeCuONC.

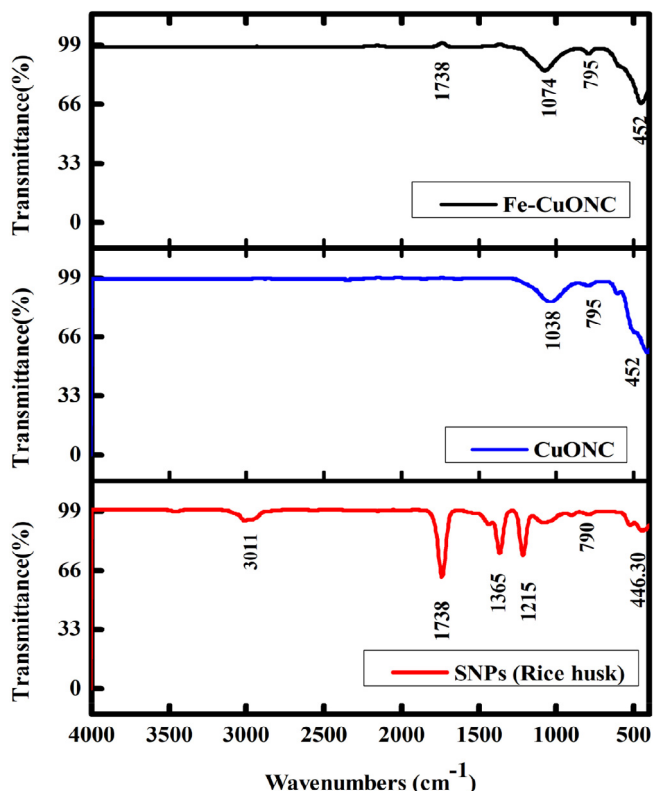


Fig. 4. FTIR analysis of SNPs, CuO NC, and FeCuONC.

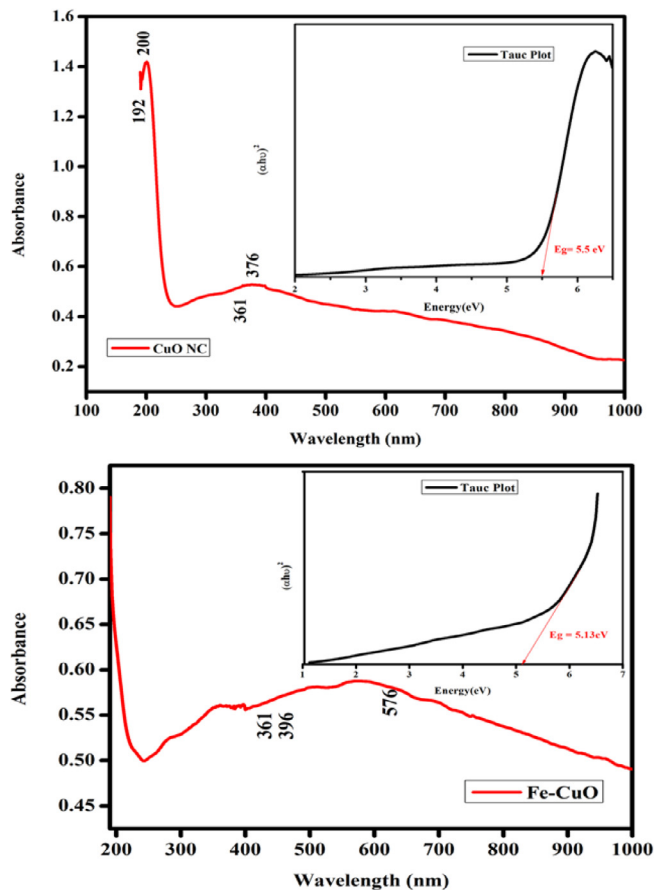


Fig. 5. Optical study CuO NC and FeCuONC.

3.4. Scanning electron microscopy characterization

Structural morphology of prepared nanostructures was visualized by scanning electron microscope (SEM) (Fig. 6). Both SNPs and CuO-SiO₂ nanocomposite (CuONC) exhibited almost needle like morphology with smooth surfaces (Fig. 6A and B). However, Fe-doped CuO-SiO₂ nanocomposites (FeCuONC) displayed the rectangular morphology with smooth surfaces (Fig. 6C). These SEM images also suggested the slight agglomeration of nanostructures. The average size of prepared nanostructures was approximately 30–70 nm which was according to XRD results. EDX was carried out to examine the elemental composition of Fe/CuO-SiO₂ nanocomposite (FeCuONC). EDX spectra indicated that Fe, Cu, Si, and O were main elements in FeCuONC without impurity (Fig. 6D). These results were in agreement with previous studies (Subhalakshmi et al. 2019).

3.5. Particle size analyzer

Particle size analyzer (PSA) was applied to examine the hydrodynamic size distribution of prepared samples (Fig. 7). The hydrodynamic diameter of prepared samples was higher than size calculated from XRD and SEM. This could be due to agglomeration of nanostructures in aqueous state (Baalousha and Lead, 2012). Fig. 7A and B indicate the optimized hydrothermal method effectively produces a well-dispersed and narrow distribution of particles diameter. Aqueous suspension of FeCuONC was fairly stable.

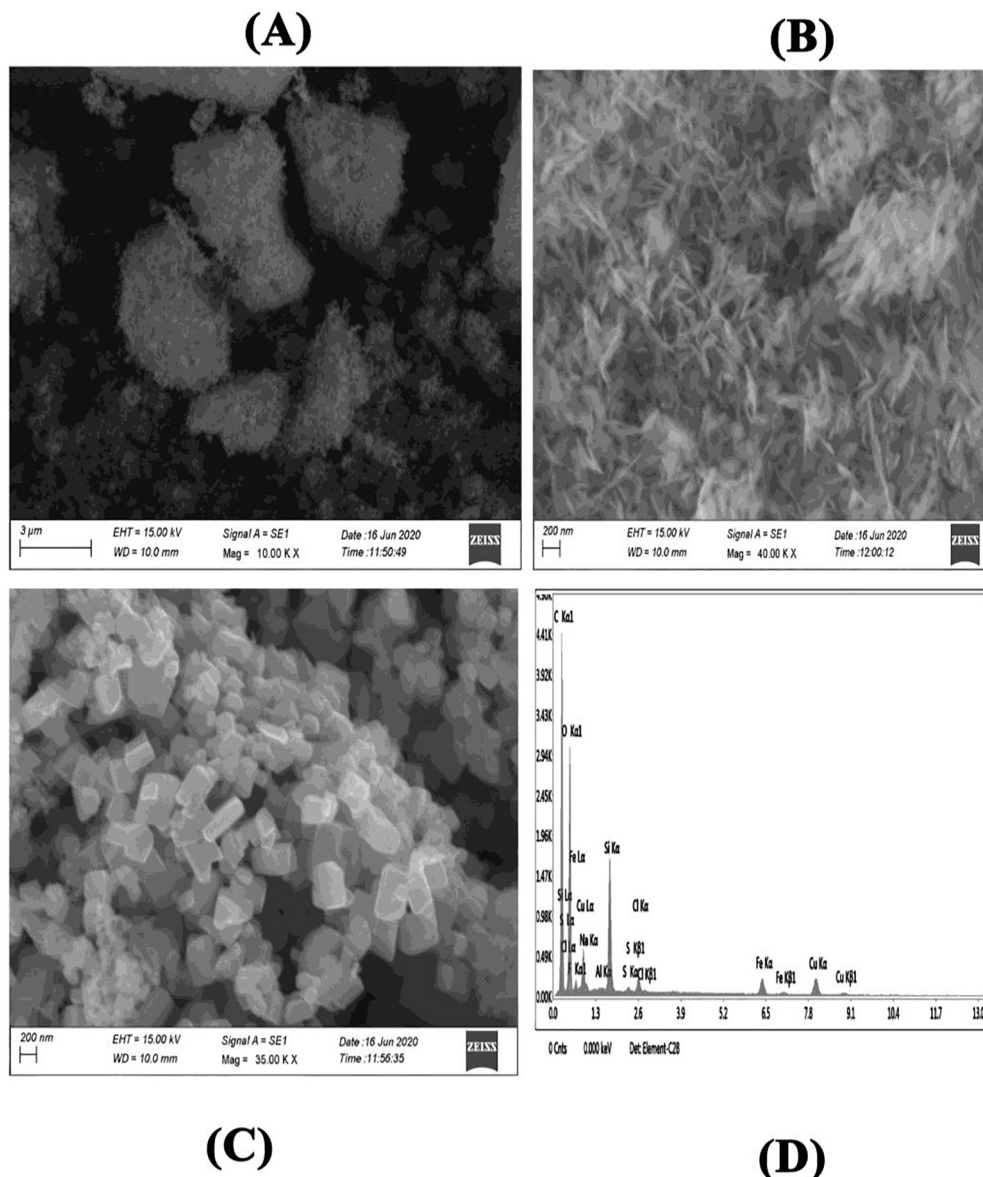


Fig. 6. SEM-EDX characterization. SEM image of SNPs (A), CuONC (B), FeCuONC (C), and SEM-EDX spectra of FeCuONC.

3.6. Thermogravimetric analysis

Thermal property of FeCuONC was analysed by TGA (Fig. 8). TGA graph predicts the 30% mass decomposition of FeCuONC 30–900 °C. The decomposition rate of FeCuONC slow as 5% weight loss per 100 °C temperature increment up to 900 °C. It expressions that 80 % thermal immovability of the complex at 900 °C. Although several studies have been carried out on the catalytic improvement of the thermal decomposition properties of FeCuONC by different nano-additives. However, that may be explained by two proposed approaches. Firstly, the higher surface area results in less sputtering of the particles during decomposition. This causes less mechanical loss and more efficient heat transfer within the nanocomposite, causing high heat release. Another reason for the

higher heat release may be attributed to the efficient combustion of NH_3 with chlorine oxides in the presence of Fe/CuO-SiO₂ nanocomposite (FeCuONC) (Joshi et al. 2008).

3.7. Antidiabetic activity

The α -amylase assay is a rapid and inexpensive technique to assess the antidiabetic activity (Laoufi et al. 2017). Antidiabetic activity of prepared samples was examined in the concentrations range of 10–50 μg/ml. Fig. 9 shows that SNPs, CuONC, and FeCuONC exhibited a concentration-dependent antidiabetic activity. Moreover, FeCuONC has highest antidiabetic activity as compared to other studied nanostructures in all tested concentrations. Hence, FeCuONC has great potential to reduce

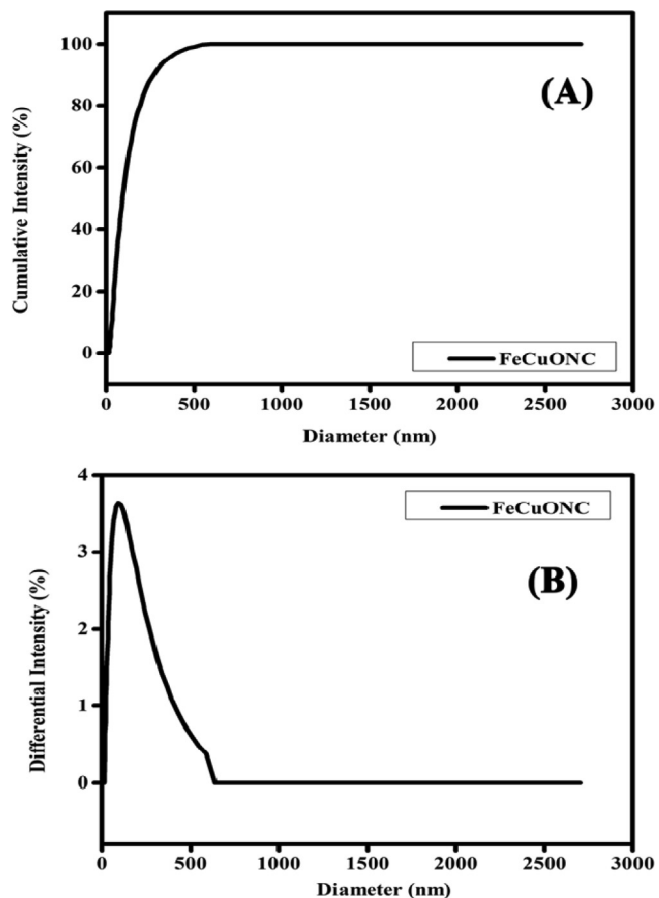


Fig. 7. Hydrodynamic size distribution of FeCuONC.

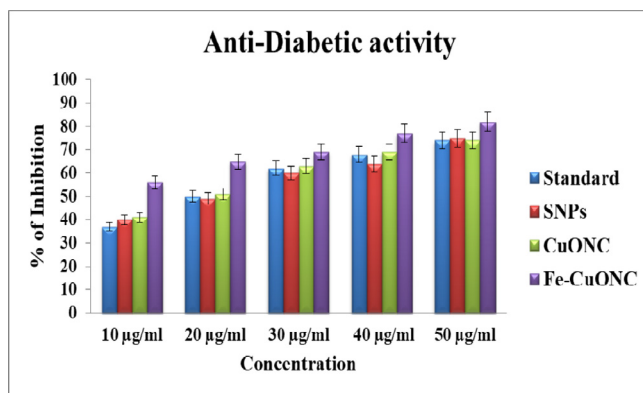


Fig. 9. Antidiabetic activity of SNPs, CuONC, and FeCuONC.

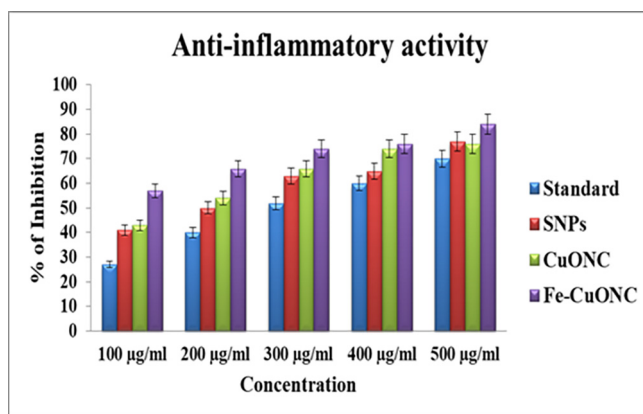


Fig. 10. Anti-inflammatory activity of SNPs, CuO NC, and FeCuONC.

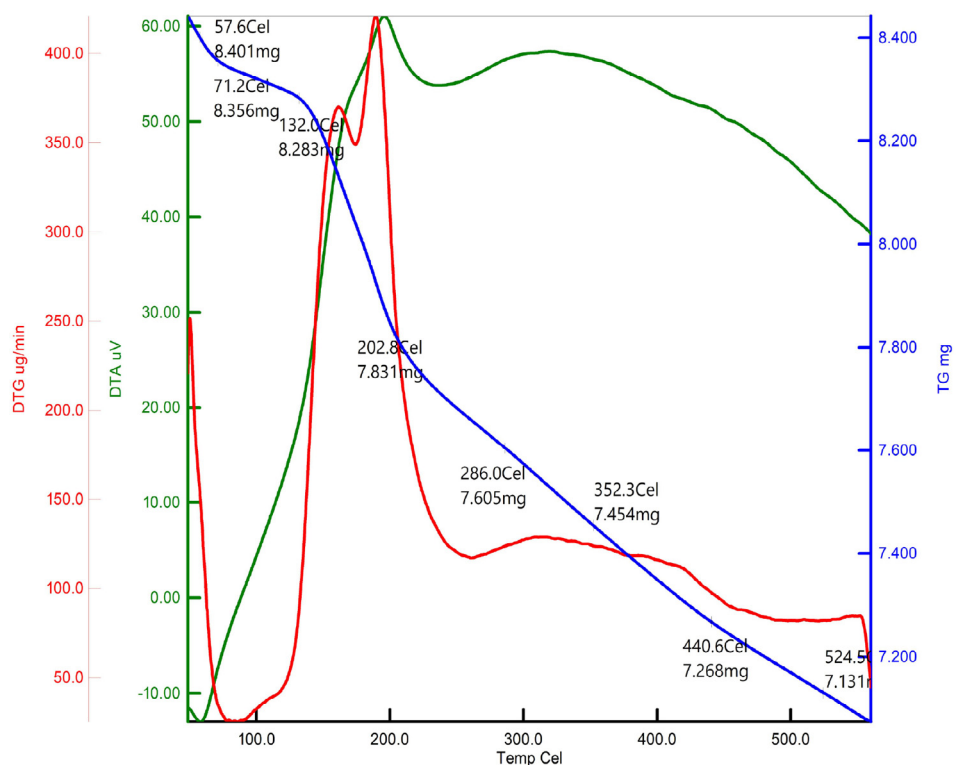


Fig. 8. TGA analysis of FeCuONC.

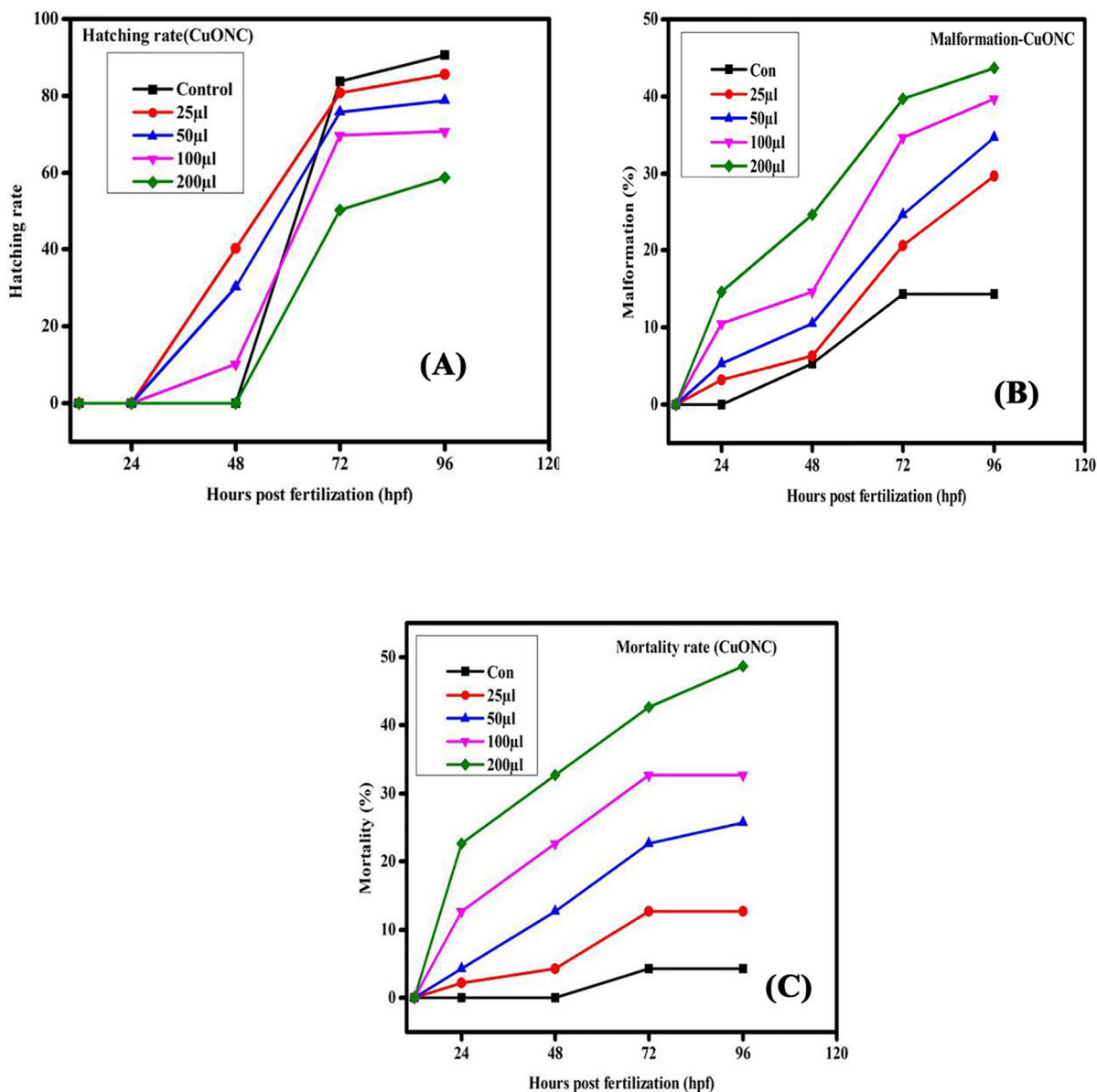


Fig. 11a. Hatching rate, malformation, and mortality rate in zebrafish embryos exposed to CuONC for different hours of post-fertilization (hpf).

the rate of digestion and absorption of carbohydrate and thereby contribute for effective management of diabetes. Our results are aligned with several recent reports that observed the antidiabetic activity of metal oxide based nanocomposites (Faisal et al., 2022; Selvan et al., 2022).

3.8. Anti-inflammatory activity

Anti-inflammatory activity (inhibition of protein denaturation) of SNPs, CuONC, and FeCuONC was assessed in the concentrations range of 100–500 µg/ml. Diclofenac sodium was used as standard materials for comparison with the inhibitory effects of prepared samples. Results showed that all three samples (SNPs, CuONC, and FeCuONC) inhibits the denaturation of egg albumins in a dose-dependent manner (Fig. 10). Moreover, FeCuONC has highest anti-inflammatory activity in comparison to studied nanostructures in all tested concentrations. Earlier studies also reported that inhibition on denaturation of egg albumin was increases with

increasing in concentration different nanostructures (Anoop and Bindu, 2015; Govindappa et al. 2011). Figs. 11a-12b

3.9. Toxicity study in zebrafish embryos and larvae

The present results represented the biological consequences and teratogenic effects of CuO-SiO₂ nanocomposite (CuONC) and Fe-doped CuO-SiO₂ nanocomposites (FeCuONC) in zebrafish. Our results are in agreement with foregoing reports on metal oxide nanocomposite toxicity in zebrafish (AshaRani et al. 2008). Aforementioned studies have employed nanocomposite of a comparable size range, but then again large surface area and the capability to produce sensitive oxygen species show a role in fashionable the toxicity of nanocomposites (Lee et al. 2007). It is also known that the toxicity varies with different capping agents (Chen et al. 2008). In this study, *in vivo* toxicity of CuONC and FeCuONC to zebrafish embryos and larvae is shown in Figs. 11 and 12. Results showed that prepared CuONC and FeCuONC deposition of on the egg surfaces increases with increasing the concen-

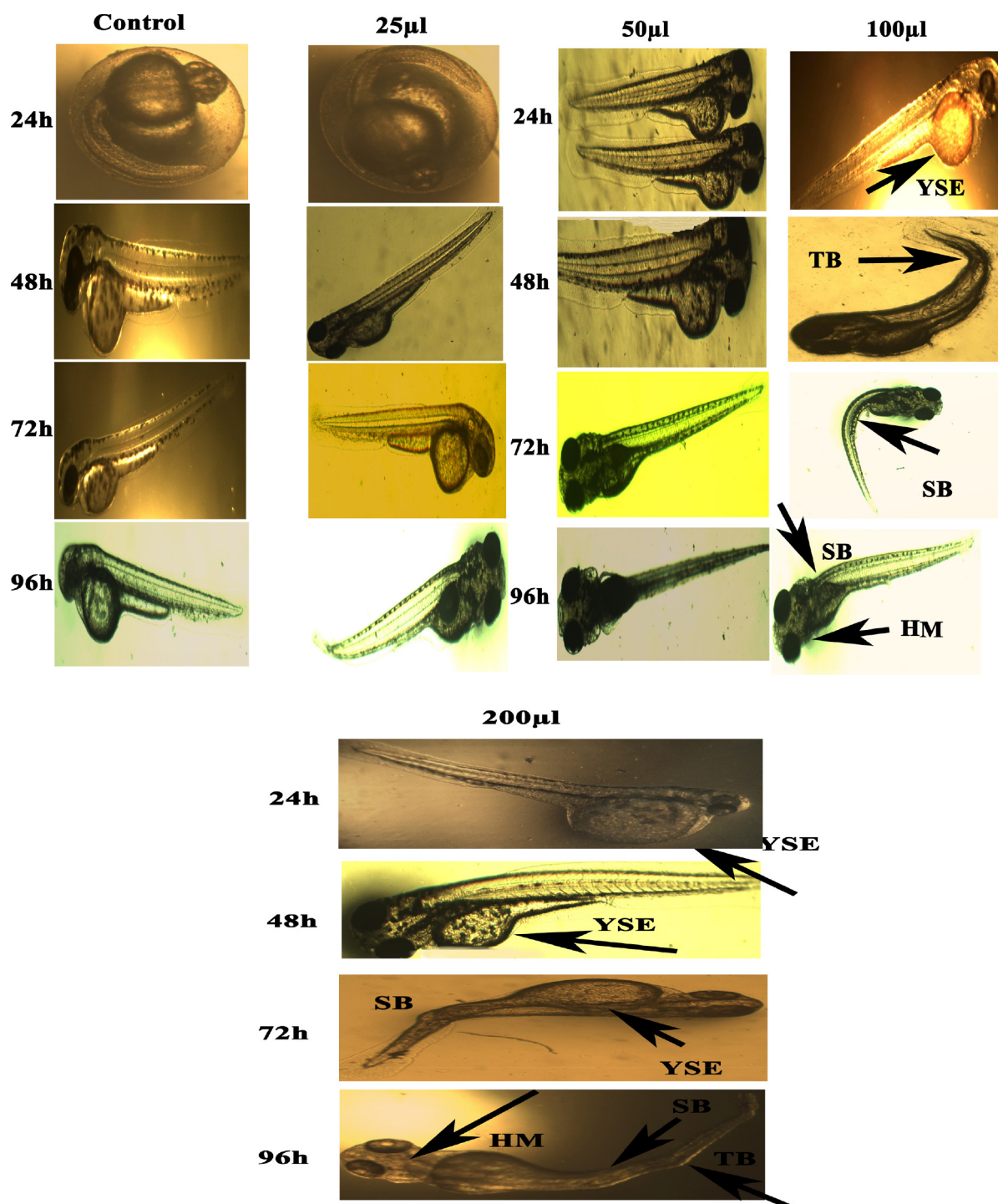


Fig. 11b. Representative images of zebrafish embryos and larvae exposed to CuONC. Control group shows the normal appearance for 24–96 hpf. Tail bent (TB), Yolk-sac edema (YSE) and head malformation (HM), and spinal card bent (SB) were markers of malformation caused by CuONC 24–96 hpf.

tration of CuONC and FeCuONC. The mortality of zebrafish embryos and larvae exposed to different concentrations (25, 50, 100, 200 $\mu\text{l/ml}$) of CuONC and FeCuONC was resolute at specific time points. The CuONC and FeCuONC at the concentration of 200 $\mu\text{l/ml}$ exhibited noticeable malformations. As shown in Fig. 11 experience in the direction of the CuONC produced embryos characteristically the malformations like spinal card bent (SB) yolk-sac edema (YSE), tail bent (TB), head malformation (HM) and delayed hatching going on the embryos of zebrafish by

the side of the higher concentration (100, 200 $\mu\text{l/ml}$) during the 24–96 hpf. The FeCuONC exhibited higher characteristic malformations comparable to the spinal cord bent (SB), yolk sac edema (YSE), tail bent (TB), head malformation (HM) and delayed hatching continuously the embryos of zebrafish at higher concentration (100, 200 $\mu\text{l/ml}$) during the 24–96 hpf. Such type of malformations was also caused by CuO NPs, ZnO NPs, ZrO-NPs, and silica NPs as reported in earlier studies (Karthiga et al. 2019; Ganesan et al. 2016). Comparable wrinkles in backbone of zebrafish

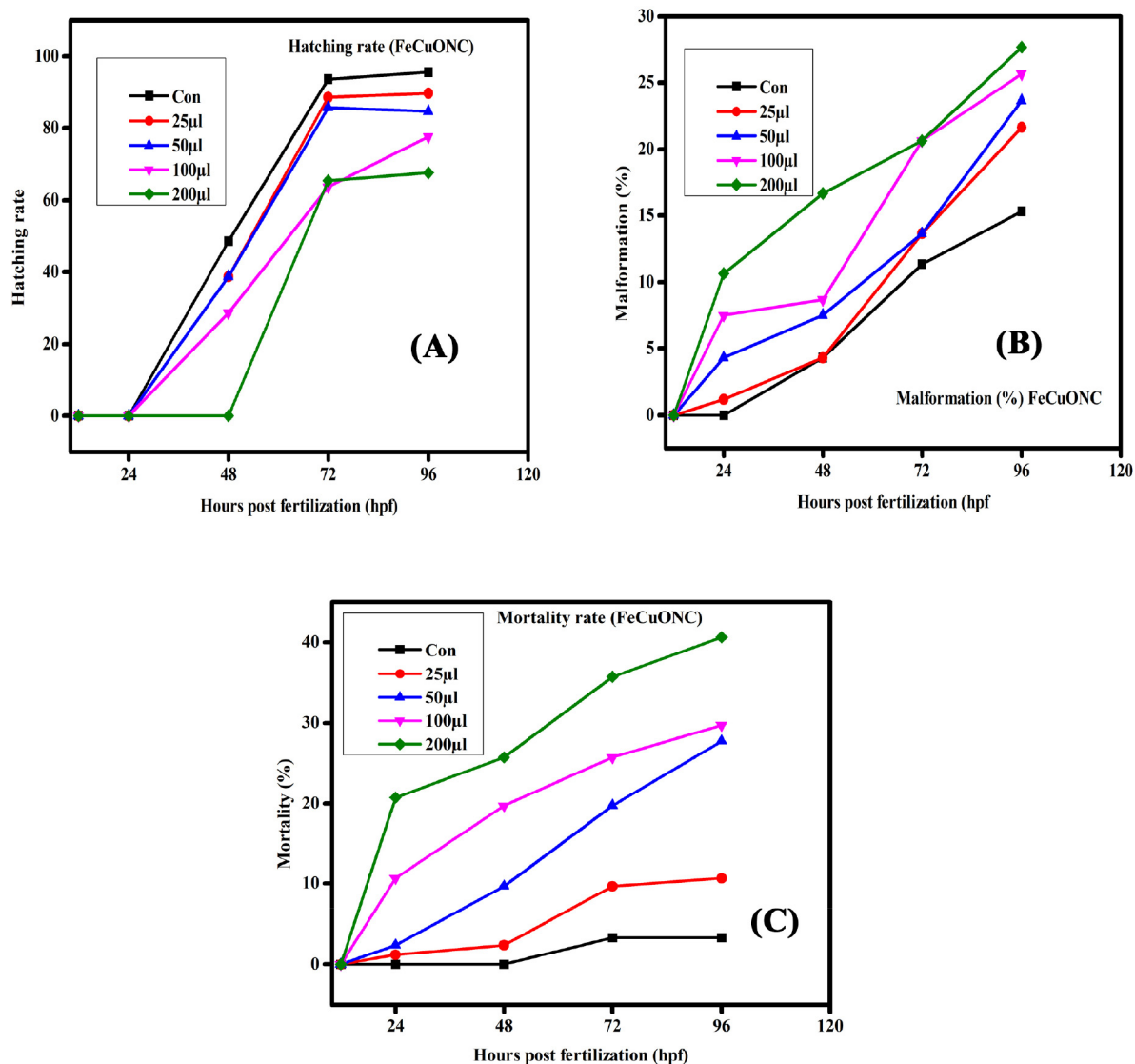


Fig. 12a. Hatching rate, malformation, and mortality rate in zebrafish embryos exposed to FeCuONC for different hours of post-fertilization (hpf).

embryos were beforehand perceived upon treatment through cadmium, where cadmium twisted somite formation consequently important to kinks and undulations (Chow and Cheng 2003). Zebrafish embryos exposed to quantum dots also demonstrated these defects (King-Heiden et al. 2009). As compared to control, CuONC and FeCuONC exposure showed the substantial

effects on mortality of zebrafish embryos. Composed 25, 50 µl/ml of CuONC and FeCuONC established toxicity, killing of 80% of zebrafish embryos at 96 hpf. Conversely 100, 200 µl/ml CuONC and FeCuONC preserved groups exhibited 100% mortality at 96 hpf. Overall, innate immunity response of FeCuONC in zebrafish was higher than CuONC

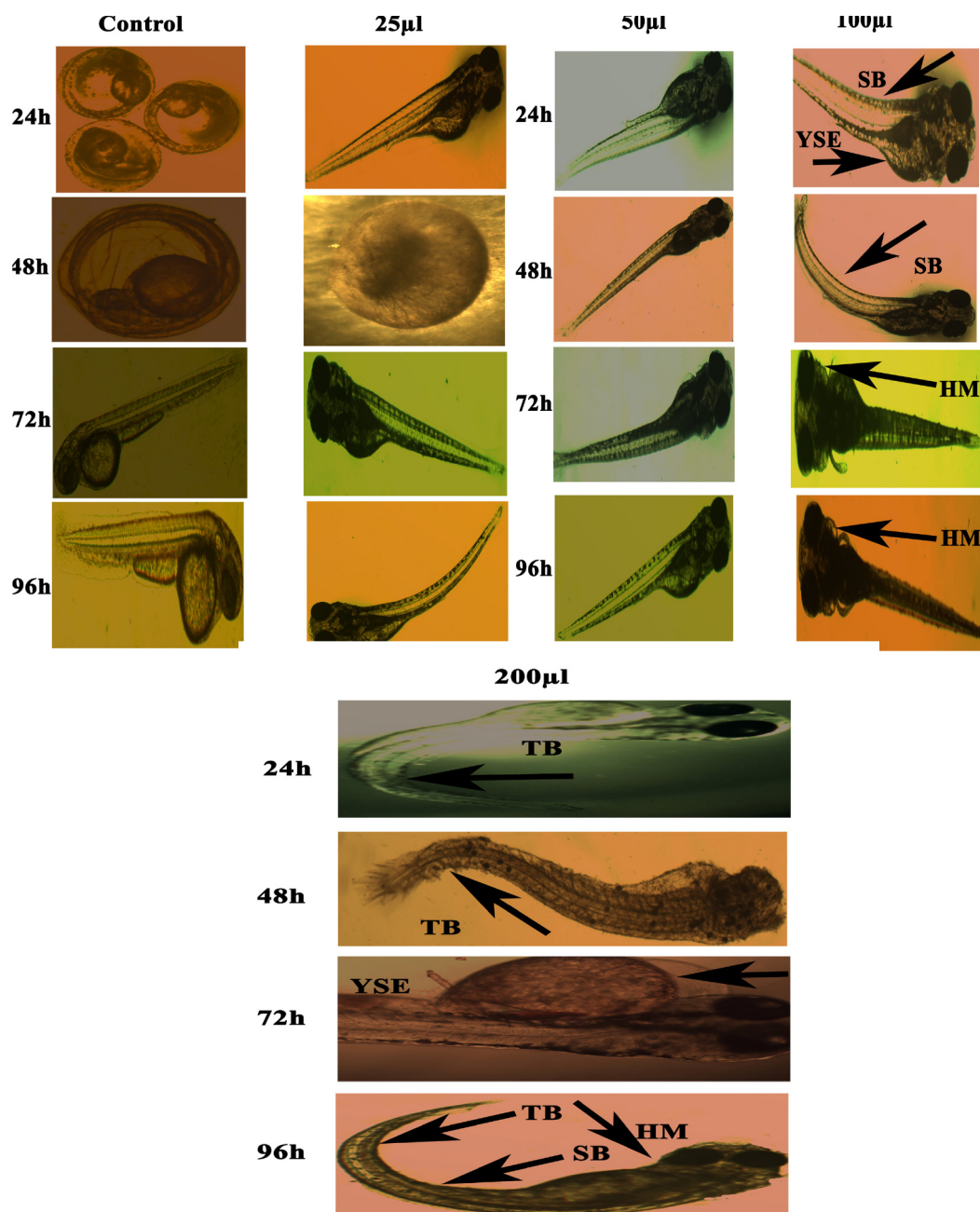


Fig. 12b. Representative images of zebrafish embryos and larvae exposed to FeCuONC. Control group shows the normal appearance for 24–96 hpf. Tail bent (TB), Yolk-sac edema (YSE) and head malformation (HM), and spinal card bend (SB) were markers of malformation caused by FeCuONC 24–96 hpf.

4. Conclusion

In vitro biological activities and *in vivo* toxicity (zebrafish) of CuO-SiO₂ nanocomposites (CuONC) and Fe-doped CuO-SiO₂ nanocomposites (FeCuONC) was assessed. The CuONC and FeCuONC were prepared by a simple hydrothermal method. The XRD, SEM, EDX, FTIR, UV-vis, PSA, and TGA were used to confirm the successful synthesis of these nanostructures. Antidiabetic potential (α -amylase assay) of FeCuONC was higher in comparison to CuONC. Anti-inflammatory effect (inhibition of denaturation of egg albumin) of FeCuONC was greater than those of CuONC. *In vivo* toxicity study in zebrafish embryos and larvae indicated that FeCuONC generated higher innate immunity response as compared to CuONC. Our data suggested that Fe-doped CuO-SiO₂ nanocomposite prepared by a simple hydrothermal method has potential

for therapeutic applications. This study warrants further research on therapeutic application of Fe-CuO-SiO₂ nanocomposites in suitable mammalian models.

Declaration of Competing Interest

The authors declare that they have no known competing financial interests or personal relationships that could have appeared to influence the work reported in this paper.

Acknowledgements

G. Sabeena (Register No: 19214542052005) acknowledges Sri Paramakalyani Centre for Excellence in Environmental Sciences, Manonmaniam Sundaranar University, Alwarkurichi – 627412,

India for providing the support for this research work. The authors extend their sincere appreciation to the Researchers Supporting Project (RSP-2021/129) at the King Saud University, Riyadh, Saudi Arabia.

References

- Adam, F., Chew, T.-S., Andas, J., 2011. A simple template-free sol-gel synthesis of spherical nanosilica from agricultural biomass. *J. Sol-Gel Sci. Technol.* 59, 580–583. <https://doi.org/10.1007/s10971-011-2531-7>.
- Ahamed, M., Akhtar, M.J., Alhadlaq, H.A., Alrokayan, S.A., 2015. Assessment of the lung toxicity of copper oxide nanoparticles: Current status. *Nanomedicine (Lond.)* 10 (15), 2365–2377. <https://doi.org/10.2217/nmm.15.72>.
- Ahamed, M., Akhtar, M.J., Khan, M.A.M., Alhadlaq, H.A., 2022a. Enhanced anticancer performance of eco-friendly-prepared Mo-ZnO/RGO nanocomposites: Role of oxidative stress and apoptosis. *ACS Omega* 7 (8), 7103–7115. <https://doi.org/10.1021/acsomega.1c06789>.
- Ahamed, M., Akhtar, M.J., Khan, M.A.M., Alhadlaq, H.A., 2021a. SnO₂-doped ZnO/reduced graphene oxide nanocomposites: synthesis, characterization, and improved anticancer activity via oxidative stress pathway. *Int. J. Nanomedicine* 16, 89–104. <https://doi.org/10.2147/IJN.S285392>.
- Ahamed, M., Alhadlaq, H.A., Khan, M.A.M., Karupiah, P., Al-Dhabi, N.A., 2014. Synthesis, characterization and antimicrobial activity of copper oxide nanoparticles. *J. Nanomater.* 2014, 637858. <https://doi.org/10.1155/2014/637858>.
- Ahamed, M., Akhtar, M.J., Khan, M.A.M., Alhadlaq, H.A., 2022b. Facile green synthesis of ZnO-RGO nanocomposites with enhanced anticancer efficacy. *Methods* 199, 28–36. <https://doi.org/10.1016/j.ymeth.2021.04.020>.
- Ahamed, M., Akhtar, M.J., Khan, M.A.M., Alhadlaq, H.A., 2021b. A novel green preparation of Ag/RGO nanocomposites with highly effective anticancer performance. *Polymers* 13 (19), 3350. <https://doi.org/10.3390/polym13193350>.
- Anoop, M.V., Bindu, A.R., 2015. In-vitro anti-inflammatory activity studies on *Syzygium zeylanicum* (L) DC leaves. *Int. J. Pharm. Res. Rev.* 4, 18–27. <https://doi.org/10.22159/ajpcr.2018.v1i4.23583>.
- Arfan, M., Siddiqui, D.N., Shahid, T., Iqbal, Z., Majeed, Y., Akram, I., Noreen, Bagheri, R., Song, Z., Zeb, A., 2019. Tailoring of nanostructures: Al doped CuO synthesized by composite hydroxide-mediated approach. *Results in Physics* 13. <https://doi.org/10.1016/j.rinp.2019.102187>.
- AshaRani, P.V., Lian, Y., Gong, Z., Valiyaveetil, S., 2008. Toxicity of silver nanoparticles in zebrafish models. *Nanotechnology* 19, (25). <https://doi.org/10.1088/0957-4484/19/25/255102>.
- Baalousha, M., Lead, J.R., 2012. Rationalizing nanomaterial sizes measured by atomic force microscopy, flow field-flow fractionation, and dynamic light scattering: sample preparation, polydispersity, and particle structure. *Environ. Sci. Technol.* 46, 6134–6142. <https://doi.org/10.1021/es301167x>.
- Chen, Y.-H., Huang, Y.-H., Wen, C.C., Wang, Y.H., Chen, W.I., Chen, L.C., Tsay, H.J., 2008. Movement disorder and neuromuscular change in zebrafish embryos after exposure to caffeine. *Neurotoxicol. Teratol.* 30, 440–447. <https://doi.org/10.1016/j.ntt.2008.04.003>.
- Chow, E.S.H., Cheng, S.H., 2003. Cadmium affects muscle type development and axon growth in zebrafish embryonic somitogenesis. *Toxicol. Sci.* 73, 149–159. <https://doi.org/10.1093/toxsci/kfg046>.
- Das, D., Nath, B.C., Phukon, P., Dolui, S.K., 2013. Synthesis and evaluation of antioxidant and antibacterial behavior of CuO nanoparticles. *Colloid. Surf. B* 101, 430. <https://doi.org/10.1016/j.colsurfb.2012.07.002>.
- Faisal, S., Jan, H., Abdullah, Alam, I., Rizwan, M., Hussain, Z., Sultana, K., Ali, Z., Uddin, M.N., 2022. In Vivo Analgesic, Anti-Inflammatory, and Anti-Diabetic Screening of *Bacopa monnieri*-Synthesized Copper Oxide Nanoparticles. *ACS Omega* 7 (5), 4071–4082.
- Farrukh, M.A., Butt, K.M., Chong, K.-K., Chang, W.S., 2019. Photoluminescence emission behaviour on the reduced band gap of Fe doping in CuO₂-SiO₂ nanocomposite and photophysical properties. *J. Saudi Chem. Soc.* 23, 561–575. <https://doi.org/10.1016/j.jscs.2018.10.002>.
- Ganesan, S., Anaimalai Thirumurthi, N., Raghunath, A., Vijayakumar, S., Perumal, E., 2016. Acute and sub-lethal exposure to copper oxide nanoparticles causes oxidative stress and teratogenicity in zebrafish embryos. *J. Appl. Toxicol.* 36 (4), 554–567.
- Garcia, G.R., Noyes, P.D., Tanguay, R.L., 2016. Advancements in zebrafish applications for 21st century toxicology. *Pharmacol. Therapeut.* 161, 11–21. <https://doi.org/10.1016/j.pharmthera.2016.03.009>.
- Govindappa, M., Naga, S.S., Poojashri, M.N., Sadananda, T.S., Chandrappa, C.P., 2011. Antimicrobial, antioxidant and in vitro anti-inflammatory activity of ethanol extract and active phytochemical screening of *Wedelia trilobata* (L.) Hitchc. *J. Pharmacogn. Phytother.* 3, 43–51. <https://doi.org/10.30799/jnpr.054.18040101>.
- Jansomboon, W., Boonmalot, K., Sukaros, S., Prapainainar, P., 2017. Rice hull micro and nanosilica: Synthesis and characterization. *Key Eng. Mater.* 718, 77–80. <https://doi.org/10.4028/www.scientific.net/KEM.718.77>.
- Joshi, S.S., Patil, P.R., Krishnamurthy, V.N., 2008. Thermal Decomposition of Ammonium Perchlorate in the Presence of Nanosized Ferric Oxide. *Def. Sci. J.* 58 (6), 271–272. <https://doi.org/10.14429/dsj.58.1699>.
- Karthiga, P., Ponnaniakamadeen, M., Rajendran, R., Annadurai, G., Rajeshkumar, S., 2019. Characterization and toxicology evaluation of zirconium oxide nanoparticles on the embryonic development of zebrafish. *Danio rerio. Drug Chem. Toxicol.* 42 (1), 104–111. <https://doi.org/10.1080/01480545.2018.1523186>.
- Khan, M.A., Singh, D., Ahmad, A., Siddique, H.R., 2021. Revisiting inorganic nanoparticles as promising therapeutic agents: A paradigm shift in oncological therapeutics. *Eur. J. Pharm. Sci.* 164. <https://doi.org/10.1016/j.ejps.2021.105892>.
- Kumari, P., Panda, P.K., Jha, E., et al., 2017. Mechanistic insight to ROS and apoptosis regulated cytotoxicity inferred by green synthesized CuO nanoparticles from *Calotropis gigantea* on embryonic zebrafish. *Sci Rep.* 7, 16284. <https://doi.org/10.1038/s41598-017-16581-1>.
- Laoufi, H., Benariba, N., Adjdir, S., Djaziri, R., 2017. In vitro α -amylase and α -glucosidase inhibitory activity of *Ononis angustissima* extracts. *J. App. Pharm. Sci* 7, 191–198. <https://doi.org/10.7324/JAPS.2017.7.0227>.
- Lee, K.J., Nallathambay, P.D., Browning, L.M., Osgood, C.J., Xu, X.H., 2007. In vivo imaging of transport and biocompatibility of single silver nanoparticles in early development of zebrafish embryos. *ACS nano* 1, 133–143.
- Liou, T.H., Yang, C.C., 2011. Synthesis and surface characteristics of nanosilica produced from alkali-extracted rice husk ash. *Mater. Sci. Eng. B* 176, 521–529. <https://doi.org/10.1016/j.mseb.2011.01.007>.
- Naatz, H., Lin, S., Li, R., Jiang, W., Ji, Z., Chang, C.H., Köser, J., Thöming, J., Xia, T., Nel, A.E., Mädlar, L., Pokhrel, S., 2017. Safe-by-Design CuO Nanoparticles via Fe-Doping, Cu-O Bond Length Variation, and Biological Assessment in Cells and Zebrafish Embryos. *ACS Nano* 11 (1), 501–515.
- Nguemngang, S.F.D., Tsafack, E.G., Mbiantcha, M., Gilbert, A., Atsamo, A.D., Nana, W. Y., Mba, V.M., Adjouzem, C.F., 2019. In Vitro Anti-Inflammatory and In Vivo Antiarthritic Activities of Aqueous and Ethanolic Extracts of *Dioscorea thollonii* Cogn. (Melastomataceae) in Rats. *Evid.-based Complement. Altern. Med.* 2019, 3612481. <https://doi.org/10.1155/2019/3612481>.
- Rahman, I.A., Vejayakumar, P., Sipaut, C.S., Ismail, J., Chee, C.K., 2009. Size-dependent physicochemical and optical properties of silica nanoparticles. *Mater. Chem. Phys.* 114, 328–332. <https://doi.org/10.1016/j.matchemphys.2008.09.068>.
- Sazegar, M.R., Dadvand, A., Mahmoudi, A., 2017. Novel protonated Fecontaining mesoporous silica nanoparticle catalyst: excellent performance cyclohexane oxidation. *RSC Adv.* 7, 27506–27514. <https://doi.org/10.1039/C7RA02280H>.
- Selvan, D.A., Kumar, R.S., Murugesan, S., Shobana, S., Rahiman, A.K., 2022. Antidiabetic activity of phytosynthesized Ag/CuO nanocomposites using *Murraya koenigii* and *Zingiber officinale* extracts. *J. Drug Deliv. Sci. Technol.* 67. <https://doi.org/10.1016/j.jddst.2021.102838>.
- T. Shahid M. Arfan A. Zeb T. BiBi T.M. Khan Preparation and physical properties of functional barium carbonate nanostructures by a facile composite-hydroxide mediated route. *Nanomater. Nanotechnol.* 8 2018 10.1177/1847980418761775 1847980418761777
- Sharifnasab, H., Alamooti, M.Y., 2017. Preparation of silica powder from rice husk. *Agric. Eng. Int: CIGR J.* 19, 158–161. <https://doi.org/10.1007/s12633-021-01611-5>.
- Siddiqui, M.A., Ahmad, J., Al-Khedhairi, A.A., Musarrat, J., Alhadlaq, H.A., Ahamed, M., 2013. Copper oxide nanoparticles induced mitochondria mediated apoptosis in human hepatocellular carcinoma cells. *PLOS ONE* 8 (8), e69534. <https://doi.org/10.1371/journal.pone.0069534>.
- Sivashanmugam, G., 2017. Antioxidant & antidiabetic activities of *Polyalthia longifolia* with special emphasis on its possible role in diabetic complications. *Int. Sch. Res. Notices.* 170.
- Subhalakshmi, N., Karunakaran, M., Kasirajan, K., Ganeshwari, N., 2019. Synthesis and characterization of different percentage (Fe²⁺) doped copper oxide (CuO) NPs prepared by chemical method. *Int. J. Sci.* 17, 22–26. <https://doi.org/10.26438/ijrsrps/v7i3.2226>.